THE ASTROPHYSICAL JOURNAL, 490:343–352, 1997 November 20

PROBING THE EQUATION OF STATE OF ULTRADENSE MATTER WITH A SUBMILLISECOND PULSAR SEARCH EXPERIMENT

L. BURDERI[1,2] AND N. D'AMICO[3,4]

Received 1996 December 11; accepted 1997 July 2

ABSTRACT

Current ideas about the equation of state for the ultradense matter constituting neutron stars provide models with a range of neutron star radii for a given mass. This implies different estimates for the maximum angular velocity that such an object could attain. The fastest and the slowest angular velocity differ by a significant amount, depending on the equation of state adopted. In particular, the identification of a submillisecond pulsar would allow us to constrain the equation of state of dense matter. In this paper, we discuss a possible evolutionary scenario resulting in a submillisecond pulsar, taking into account current ideas about the evolution of the magnetic field of neutron stars. Pulsar luminosities and lifetimes in the submillisecond period range, derived on the basis of phenomenological considerations, suggest that the effort of searching for such an object would be worthwhile. All the pulsar searches conducted up to now have been prevented by instrumental selection effects from probing the submillisecond range. We discuss the feasibility of a submillisecond pulsar search experiment in the context of current hardware and software capabilities.

Subject headings: dense matter — equation of state — pulsars: general — radio continuum: stars — stars: neutron

1. INTRODUCTION

The detection of the shortest rotation period of a neutron star (NS) can be used to test the equation of state (EOS) of dense matter. The basic structure of a NS, and hence its minimum rotation period, depends on the EOS adopted to describe the behavior of nuclear matter at very high densities ($\geq$ nuclear matter densities $\sim 10^{14}$ g cm^{-3}).

In the context of the standard gravitationally bound NS model, several EOSs were proposed, implying different stiffnesses for the nuclear matter constituting NSs. The most relevant difference between the various equations is in the predicted radius of the NS. For a star of fixed baryon number, the softer equations predict smaller radii and hence significantly shorter minimum rotation periods. If the EOS is very stiff, the minimum rotation period for a NS is around 1.6 ms, very close to the minimum observed 1.56 ms for PSR B1937+21. If the EOS is very soft, the minimum period can easily be below 1 ms. The coincidence of the minimum observed period with the lower limit of the stiffest EOS is rather intriguing. However, we will show that instrumental selection effects of current pulsar searches have prevented sampling of the short period range ($\leq$1.5 ms).

Recently, based on few minimal constraints, a minimum period for a gravitationally bound object has been found (Glendenning 1992; Koranda, Stergioulas, & Friedman 1997). Furthermore, in the case of a self-bound star like a strange star (Glendenning 1992), the minimum spin period can be even shorter. The hypothetical detection of such a short period could be used to probe the ground state of the baryon matter.

Phinney & Kulkarni (1994) discussed some implications of the existence of a submillisecond pulsar for the EOS of ultradense matter, for the evolutionary scenarios proposed for some of the binary systems containing a millisecond pulsar, and for the general theory of relativity. Here we adopt a more phenomenological approach and discuss the possibility of detecting such an object in terms of present hardware and software resources. Although the stability of a submillisecond pulsar requires a relatively small NS radius, the possibility of the existence of such an object and its detectability depend on three basic conditions: (1) the efficiency of a suitable formation process, (2) the resulting pulsed luminosity, and (3) the lifetime spent as a submillisecond pulsating source. A systematic search for submillisecond pulsars is a major task and requires specialized hardware and software facilities. On the other hand, the results of such a search might have a strong impact on the understanding of the EOS of dense matter, so it is important to evaluate when the conditions mentioned above can be satisfied.

In this paper we speculate on the basis of current ideas about the millisecond pulsar formation process that one consequence of the presence of a smaller radius NS could be the formation of a submillisecond, medium luminosity, relatively long-lived radio pulsar. Indeed, we demonstrate that most of the present surveys are strongly biased against the detection of such objects, and we discuss the improvements required to overcome this bias. In § 2 we briefly review the various equations of state and their predictions for the internal structure of a NS, for its relativistic Keplerian frequency (i.e., the rotational frequency of a test particle orbiting at the NS equator that sets the upper limit to the NS rotation against centrifugal disruption) and for the lower limits to the rotation period set by nonaxisymmetric instabilities. In § 3 we review the recycling model, discuss the potential role of the magnetic field decay of an accreting NS in the formation process of millisecond and submillisecond pulsars, and attempt to estimate the luminosity and lifetime of a potential submillisecond pulsar. In § 4 we compare

[1] Astronomy Group, University of Leicester, Leicester LE1 7RH, U.K.; lbu@star.le.ac.uk.
[2] Istituto di Fisica dell'Università, via Archirafi 36, 90123 Palermo, Italy.
[3] Osservatorio Astronomico di Bologna, via Zamboni 33, 40126 Bologna, Italy.
[4] Istituto di Radioastronomia del CNR, via Gobetti 101, 40129 Bologna, Italy.

these results with the hardware and software capabilities of a pulsar search experiment.

2. THE ROTATING NEUTRON STAR STRUCTURE

The equation of state of the ultradense matter determines the NS structure and its behavior under rapid rotation. Depending on the EOS adopted, the NS can be a gravitationally bound object in which the ultradense matter is held together by the action of gravity (as in the "classical" neutron-matter EOS, see, e.g., Stergioulas & Friedman 1995; Cook, Shapiro, & Teukolsky 1994), or a self-bound object in which the ultradense matter is self-confined in a stable state (see, e.g., Witten 1984; Glendenning 1992).

For a given baryon mass and EOS, a firm lower limit to the spin period is given by its stability under the action of centrifugal forces. In § 2.1 we show how this condition could, in principle, discriminate between a gravitationally bound and a self-bound object. On the other hand, a realistic estimate of the minimum allowed rotation period must carefully take into account the effects of instabilities arising in a rapidly rotating fluid spheroid. As an example, in § 2.2 we consider these effects on two neutron-matter EOSs.

In § 3 we apply some relations derived in a nonrelativistic (Newtonian) context (e.g., the Alfvén radius) to the space close to an intrinsic relativistic object such a submillisecond pulsar. In order to justify this approach, it is worth discussing in more detail the relativistic and dynamical effects of fast rotation on NS structure. In § 2.1 we show that, with a reasonable accuracy, we can discuss the physical processes occurring near the surface of a rapidly rotating NS in a classical Newtonian context, provided that we take into account the inflation of its radius due to the rapid spin. Moreover, all other special relativistic effects can be neglected in a first approximation, as the Lorenz factor is ~ 1.1 for speeds of $\sim(2\pi/P_{\rm K,eff})R(P_{\rm K,eff})$, where $P_{\rm K,eff}$ is the minimum spin period before centrifugal disruption (see below) and $R(P_{\rm K,eff})$ is the corresponding NS radius.

2.1. *The Relativistic Keplerian Period of a Neutron Star*

Without entering into detailed calculations of the relativistic effects for the effective minimum spin period before centrifugal disruption for a rotating NS, we note that most of the numerical computations based on a gravitationally bound neutron-matter EOS converge toward a similar value, given by the relation

$$P_{\rm K,eff} = 1.75 P_{\rm K} , \tag{1}$$

where $P_{\rm K} = 2\pi(GM_0/R_0^3)^{-1/2}$ is the classical Keplerian angular frequency of a test particle orbiting at the equator of a nonspinning NS of the same baryon mass, M_0 being its gravitational mass (i.e., the total gravitational mass-energy of the NS), and R_0 being its circumferential equatorial radius (i.e., the *proper* circumference in the equatorial plane divided by 2π). The factor 1.75 takes into account all the relativistic and dynamical effects, and G is the gravitational constant. This formula is accurate to within $\sim 20\%$ for the EOS discussed in Friedman, Ipser, & Parker (1986) and more recently in Cook et al. (1994). The values of M_0 and R_0 for a given baryon mass are listed in the same paper. For a wide range of baryon masses and EOSs, their results agree to within 5% with the values given by Lindblom (1986), based on different numerical computations (Lindblom & Detweiler 1977; Detweiler & Lindblom 1985). Table 1 summarizes the results of Cook et al. (1994) for one of the stiffest (gravitationally bound) EOSs, i.e., the Mean Field (Pandharipande & Smith 1975), labeled L by Arnett & Bowers (1977), and one of the softest (gravitationally bound) EOSs, i.e., the Reid core with hyperons (Pandharipande 1971), labeled B. Comparing EOSs L and B we conclude the following:

1. Decreasing the spin period from infinity (nonrotating NS) to $P_{\rm K,eff}$ increases the equatorial radius of both models by $\sim 50\%$.
2. The difference in equatorial radii between the models is about a factor of 2 over the full range of rotational periods.
3. The gravitational masses are constant (within 5%) throughout the period range for a given EOS and baryon mass M_b (the rest mass of the same number of baryons, where the rest mass per baryon is taken as 1.59×10^{-24} g, to agree with the conventions of Arnett & Bowers 1977).

In Figure 1, we plot $\Omega_{\rm K,eff} = 2\pi/P_{\rm K,eff}$ as computed by Cook et al. (1994) for $M_b = 1.4\ M_\odot$ models against the quantity M/R^3 for 13 different EOSs, where the circumferential equatorial radius is computed for $P = P_{\rm K,eff}$. The solid line is the Keplerian line defined by $P = 2\pi(GM/R^3)^{-1/2}$. It is immediately evident that to a very good

TABLE 1

NEUTRON STAR PROPERTIES FOR TWO EXTREME NEUTRON-MATTER EQUATIONS OF STATE

	$M = 1.4$					$M_b = M_{b\,\max}$				
EOS	ω	R	M	M_b	e	ω	R	M	M_b	e
B	0.00	...	1.40	1.61	0.000	0.00	7.04	1.41	1.63	0.000
	1.17	11.10	1.45	1.61	0.785	1.19	11.00	1.46	1.63	0.784
L	0.00	14.99	1.40	1.52	0.000	0.00	13.70	2.70	3.23	0.000
	0.45	21.25	1.47	1.52	0.813	0.65	20.66	2.81	3.23	0.812

NOTE—Variations of gravitational mass, circumferential equatorial radius (R in km), and eccentricity, with angular speed ω in units of 10^4 s^{-1} (ranging from 0.0 to $\omega_{\rm K,eff}$) for NSs with fixed baryon masses for a given EOS. M and M_b are the gravitational and baryon masses, respectively, in units of solar masses. $M_{b\,\max}$ is the maximum allowed baryon mass for a nonspinning NS with a given EOS. The eccentricity is defined from the ratio of the proper polar to equatorial radii: $1 - e^2 = (R_p/R_{\rm eq})^2$ (see Cook et al. 1994). Data is from Cook et al. 1994. For EOS B, the value for the radius of the nonrotating $M = 1.4\ M_\odot$ NS is not reported, but it probably does not differ too much from the case of a nonrotating $M_{b\,\max}$.

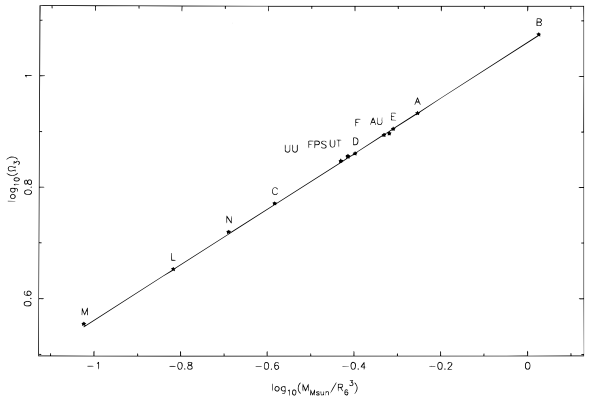

FIG. 1.—Limiting angular velocity for 1.4 $M_\odot$ NS corresponding to the 13 EOSs investigated by Cook et al. (1994) and labeled after Arnett & Bowers (1977). The solid line is the classical Keplerian angular velocity for a particle orbiting at the (rotationally inflated) NS equator. Ω_3 is the angular velocity in units of 10^3 radiant s^{-1}.

approximation, the minimum allowed spin period for a NS occurs when its equatorial speed reaches the *classical* Keplerian limit for the given equatorial radius and gravitational mass. In this approximation, the rapid rotation inflates and deforms ($e > 0$) the NS surface and slightly increases its gravitational mass. While the non–spherically symmetric deformations (oblateness effects) are important in determining the radius of the spinning NS, they are almost irrelevant in changing the gravitational field felt by a test particle at the NS equator with respect to the corresponding spherical configuration. This is probably due to the fact that most of the mass is concentrated well inside the external radius, where the deformation effects arising from rotation are almost negligible. In this respect, the correction factor of 1.75 used for obtaining $P_{\rm K,\,eff}$ from $P_{\rm K}$ is mainly determined by the $\sim 50\%$ increase of the NS radius for *any* EOS. In fact, we have $[R(P_{\rm K,\,eff})/R_0]^{3/2} \sim (1.5)^{3/2} = 1.84$, consistent with our empirical value of 1.75. This agrees with the prediction of the so-called Roche model (see, e.g., Shapiro & Teukolsky 1983). This model assumes that the distribution of most of the mass of the NS is unchanged by the rotation, and concludes that the maximum expansion of a uniformly rotating star along its equator is a factor of 3/2.

For a given baryon mass, different gravitationally bound EOSs predict different radii for the nonspinning equilibrium configuration. The largest radii correspond to the stiffest EOS, the smallest to the softest. It is clear from equation (1) that the softest EOSs allow the shortest spin periods. Parametrizing the various possible EOSs describing a gravitationally bound, neutron-matter NS, and adopting an empirical formula for the minimum spin period similar to our relation in equation (1) or numerical models of rapidly rotating NSs, Glendenning (1992) and Koranda et al. (1997) searched for the EOS that would minimize the rotational period for a given mass. Since the object is gravitationally bound, its radius is a decreasing function of the mass (for a pure neutron gas, $R \propto M^{-1/3}$). Together with equation (1), this implies that the EOS that will minimize the period for a given maximum allowed mass for a nonrotating NS ($M_{0\,\rm max}$) will allow the most centrally condensed star while still supporting a mass $M_{0\,\rm max}$. For *any* gravitationally bound EOS satisfying only few reasonable restrictions, such as nonviolation of the causality, Koranda et al. (1997) found a numerical relation for the minimum period of a gravitationally bound NS in terms of $M_{0\,\rm max}$ given by

$$P_{\rm GBound} \geq 0.288 + 0.20\left(\frac{M}{M_\odot} - 1.442\right) \text{ ms} . \qquad (2)$$

Under a slightly different hypothesis, Glendenning (1992) found a result in agreement to within 15%. On the other hand, for a self-bound object, such a limit does not hold. The firm lower limit is set by the requirement of the stability of the NS with respect to Einstein's equations of general relativity and by equation (1),

$$P_{\rm SBound} \geq 0.167\left(\frac{M}{M_\odot}\right) \text{ ms} \qquad (3)$$

(Glendenning 1992). Both of these limits are probably underestimates, as there is no physical reason that requires that the true EOS should minimize the rotational period. Nevertheless, the detection of a submillisecond pulsar with a period in the range delimited by equations (2) and (3) at the largest accurately measured mass of a NS ($\sim 1.442\ M_\odot$; Taylor & Weisberg 1989) would demonstrate unambiguously the self-bound nature of the ultradense matter.

2.2. *Nonaxisymmetric Instabilities of a Rotating Neutron Star*

Nonaxisymmetric instabilities arise in a rapidly rotating fluid spheroid. The modes of oscillation of such a spheroid spinning at angular speed ω show the dependence

$$\exp\left[i\sigma_m(\omega)t + im\phi - t/\tau_m(\omega)\right] , \qquad (4)$$

where $i = 1^{-1/2}$, t and ϕ are the time and the azimuthal angle, m is an integer that characterize the mode, $\sigma_m(\omega)$ is the mode frequency, and $\tau_m(\omega)$ is a suitable constant related to the growing or damping timescale of the mode. These modes are damped if $\tau_m > 0$ and instabilities occur when τ_m becomes < 0. The critical frequency ω_m at which a particular instability sets in can be obtained by solving the equation $\tau_m^{-1}(\omega_m) = 0$. Two kind of instabilities may occur, corresponding to positive or negative $|m| \geq 2$ modes. The instabilities of the $m \leq -2$ modes are driven by the viscosity of the fluid and were investigated first in the 19th century by Kelvin (see, e.g., Thomson & Tait 1883) in the context of an incompressible fluid (Maclaurin spheroid). The instabilities of the $m \geq +2$ modes are driven by gravitational radiation (GR) and were first investigated, for the Maclaurin spheroids, by Chandrasekar (1970a, 1970b). More recently, Comins (1979a, 1979b) studied both of these effects. Later, these oscillations were investigated in the context of Newtonian polytropes and more realistic NS models by several authors, e.g., Friedman (1983), Imamura, Durisen, & Friedman (1985), Managan (1985), Lindblom (1986, 1987), Cutler & Lindblom (1987), Cutler, Lindblom, & Splinter (1990), and Mendell (1991); see Friedman & Ipser (1992) for a review. The main results of these investigations can be summarized as follows:

1. The positive m modes are driven by GR and damped by viscosity, the reverse holding for negative m modes.
2. Above 2×10^{10} K, the bulk viscosity damps all the modes.
3. For GR-driven modes with $m > 5$, the viscous timescale is shorter than the GR timescale for NS temperatures

$T \leq 10^{10}$ K, so all the $m > 5$ modes are damped by viscosity for realistic temperatures of the NS.

4. For 10^7 K $< T < 10^9$ K, the situation is unclear. In principle, this is the range of temperatures at which the $m \geq +2$ instabilities set in. The related frequencies were computed by Cutler & Lindblom (1987) for a range of temperatures and different EOSs. However, Mendell (1991) claims that below the superfluid transition temperature of the NS matter ($\sim 10^9$ K), the effects of "mutual friction" (i.e., the friction between electrons and neutron vortices) are large enough to damp the nonaxisymmetric instabilities.

5. For $T < 10^7$ K, the viscosity of the NS is so high that all the positive modes, $m = 2$, 3, 4, and 5, are damped out by viscosity (Lindblom 1987).

6. In the context of the viscosity-driven modes, the smallest angular speeds at which these instabilities set in occurs for the $|m| \leq 5$ modes. The frequencies at which the $m \leq -2$ instabilities set in depend on the NS temperature. These limit frequencies, for $T = \infty$ and $T = 0$ K, were computed for different EOSs by Lindblom (1987).

7. For $T < 10^7$ K, the NS centrifugal frequency is usually lower than the smallest frequencies at which both the instabilities set in.

Therefore, for a given NS temperature, the minimum allowed rotational period, $P_{\rm lim}$, is the maximum of the centrifugally limited ($P_{\rm K,eff}$) and the periods of the nonaxisymmetric instabilities effective for that temperature. As an example, Figure 2 shows the resulting minimum rotation period for the two EOSs discussed before as a function of the NS temperature. For the full range of temperatures shown, the period at which the rotation of the NS becomes unstable is practically constant for a given EOS and baryonic mass. For a realistic range of NS temperatures, the derived values are remarkably close to those determined by the centrifugal limit $P_{\rm K,eff}$. It is worth noting that the results for the two extreme gravitationally bound EOSs differ substantially, so the detection of a submillisecond pulsar could be used as a probe to discriminate between the two cases.

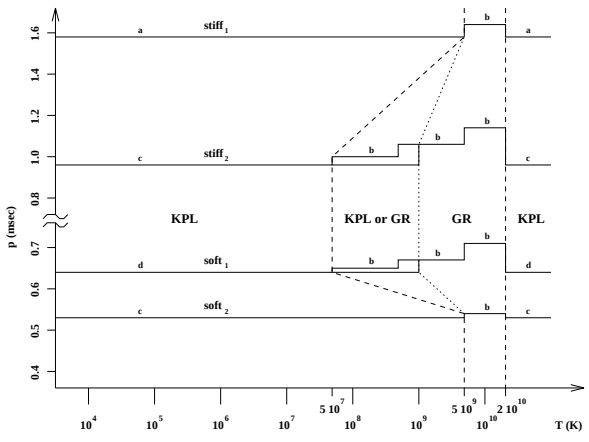

FIG. 2.—Schematic plot of the shortest possible periods for a rotating NS vs. the NS temperature. Curves labeled soft$_1$ and soft$_2$ refer to EOS B and baryon masses of $M_{\rm b} = 1.4\ M_\odot$ and $M_{\rm b\,max} = 1.63\ M_\odot$, respectively; curves labeled stiff$_1$ and stiff$_2$ refer to EOS L and baryon masses of $M_{\rm b} = 1.4\ M_\odot$ and $M_{\rm b\,max} = 3.23\ M_\odot$, respectively. KPL indicates the zones, delimited by the first and the last dashed line, where the minimum period is determined by the centrifugal instabilities. GR indicates the zone where the minimum period is determined by the gravitational radiation–driven instability. In the zone between the left dashed line and the dotted line, KPL may be the limiting instability if mutual friction damps the GR instability. (*a*) From Friedman et al. (1986); (*b*) from Cutler & Lindblom (1987); (*c*) from Cook et al. (1994); (*d*) from Friedman & Ipser (1992).

3. THE FORMATION OF A MILLISECOND PULSAR

The most widely accepted scenario for the formation of a millisecond pulsar is the recycling of an old NS by a spin-up process driven by accretion from a binary companion (for a review, see Bhattacharya & van den Heuvel 1991). In this model, as a result of the nuclear evolution of the companion, the NS eventually accretes matter overflowing the companion's Roche lobe, which thus has enough specific angular momentum to form a Keplerian accretion disk. The Alfvén radius $R_{\rm A}$ of a magnetized accreting NS is defined as the radius at which the (assumed dipolar) NS magnetic field pressure equals the ram pressure of the spherically accreting (free-falling) matter,

$$\frac{B(R_{\rm A})^2}{8\pi} = \rho(R_{\rm A}) v_{\rm ff}(R_{\rm A})^2 \ , \qquad (5)$$

where B is the NS magnetic field, and ρ and $v_{\rm ff}$ are the density and the free-fall speed of the accreting matter. The accretion radius r_a is ϕ times the Alfvén radius, where the factor $\phi \sim 1$ depends on the details of the accretion process. Outside this radius, the accreting matter is assumed not to be influenced by the magnetic field, while well inside it, it is assumed to follow the field lines. Using the continuity equation for $\rho(r)$, one finds that

$$r_a = 1.0 \times 10^6 (\phi \mu_{26}^{4/7} \dot{m}^{-2/7} M^{-1/7} R_6^{-2/7})\ {\rm cm} \ , \qquad (6)$$

where μ_{26} is the magnetic moment ($\mu = B_{\rm surface} R^3$) in units of 10^{26} G cm^3, $\dot{m}$ is the accretion rate in Eddington units (for a 10^6 cm stellar radius the Eddington accretion rate is $1.5 \times 10^{-8}\ M_\odot\ {\rm yr}^{-1}$), and R_6 is the NS circumferential equatorial radius in units of 10^6 cm. The accreting matter couples to the NS magnetic field at the accretion radius r_a. In this way, the pulsar accretes angular momentum, and spins up. This process ends when the NS is spinning at about the same angular speed as the Keplerian matter at the accretion radius; any further spin-up results in a centrifugal inhibition of the accretion. Once this equilibrium period is attained, the accretion proceeds with a constant NS spin. After the accretion phase, the pulsar is visible as a very fast, low-field NS: a millisecond pulsar. The equilibrium spin period can be derived from the Kepler relation $2\pi/P_{\rm eq} = f_s (GM)^{1/2} r_a^{-3/2}$, where $f_s \leq 1$, the fastness parameter, equals 1 if the pulsar is spinning at exactly the Kepler speed of the accreting matter,

$$P_{\rm eq} = 0.57 (\phi^{3/2} f_s^{-1} \mu_{26}^{6/7} \dot{m}^{-3/7} M^{-5/7} R_6^{-3/7})\ {\rm ms} \ . \qquad (7)$$

Two constraints apply to equation (7): (1) the accretion radius computed via the relation of equation (6), from which equation (7) has been derived, cannot be smaller than the NS radius R, and (2) the nonaxisymmetric instabilities discussed in the previous section could keep the NS spin in a different equilibrium state, where the excess of angular momentum accreted onto the NS is radiated away (e.g., by the emission of gravitational radiation).

Taking these effects into account, the equilibrium spin period attainable in this way is given by the relation

$$P_{\rm eq} = \max\left\{ \frac{2\pi}{f_s (GM)^{1/2}} [\max\ (r_a, R)]^{3/2}, P_{\rm lim} \right\} . \qquad (7a)$$

3.1. *Current Ideas on the Magnetic Field Decay of an Accreting Neutron Star*

The magnetic moment of a radio pulsar is measured with the relation

$$\mu = 3.2 \times 10^{37}(P\dot{P})^{1/2} \text{ G cm}^3 , \quad (8)$$

where $\dot{P}$ is the NS period derivative. The magnetic moments measured in millisecond binary pulsars are substantially lower than the typical single-pulsar value of 10^{29}–10^{31} G cm^3, and are all crowded around 10^{26} G cm^3 (for a review, see Bhattacharya & van den Heuvel 1991). The standard scenario originally assumed that magnetic moments decayed exponentially on timescales of a few million years (Ostriker & Gunn 1969), but more recent statistical studies suggest that no significant magnetic moment decay occurs on a timescale of 100 million yr (Bhattacharya et al. 1992; Wakatsuki et al. 1992). However, the question of whether magnetic moment decay actually occurs in NSs is still open (for a review, see Bhattacharya & Srinivasan 1995). Theoretical studies of NSs with magnetic fields anchored in the crust or more deeply in the superfluid core seem to indicate that spontaneous field decay is unlikely (Sang & Chanmugam 1987; Urpin & Muslimov 1992). To explain the low values of the magnetic moments of millisecond pulsars, some theories consider the idea that the accretion of matter onto the NS before it becomes a radio pulsar causes the magnetic field to decay (Bisnovatyi-Kogan & Komberg 1974; Taam & van den Heuvel 1986; Blondin & Freese 1986; Shibazaki et al. 1989). More recently, based on observational evidence, some authors suggest the possibility of a minimum ("bottom") value for the magnetic moment of a NS, below which any decay stops (Kulkarni 1986; Romani 1990; van den Heuvel & Bitzaraki 1994; van den Heuvel 1995; Burderi, King, & Wynn 1996). Romani (1990) proposed that during the initial stage of accretion, when the NS surface magnetic field is very strong ($B_{\text{surface}} \geq 10^9$ G), the accretion process follows the standard picture, in which the accreting matter is funneled by the dipolar magnetic field toward the NS magnetic poles. There, the static pressure p of the material in the accretion column just above each magnetic pole is so high ($p \geq B^2_{\text{surface}}/8\pi$) that the matter is no longer confined by the magnetic field and is forced to move sideways to settle down near the NS equator. The density of the matter is so high that it is very efficiently coupled to the magnetic field. This implies that the matter carries away the magnetic field lines toward the NS equator, where they are advected below the surface and screened by the diamagnetic accreted material, causing the field intensity to decrease. For $B_{\text{surface}} \leq 10^9$ G, the density of the matter in the accretion column at which the pressure is $\geq B^2_{\text{surface}}/8\pi$ is 1–10 g cm^{-3}. For these density values, the ohmic decay and the fluid interchange timescales are shorter than the settling timescales ($\sim$free-flow timescale). In this case, the material no longer drags the magnetic field, causing the field decay to stop. Hence this model predicts

$$\mu_{\text{bot}} \sim 10^{27} R_6^3 \text{ G cm}^3 \quad (9)$$

for the bottom value of the magnetic moment of the NS. The idea that magnetically funneled accretion causes the magnetic field to decay has also been discussed by van den Heuvel (1995) and Burderi et al. (1996). An interesting point raised by these authors is that for standard values of the NS radius and mass and for accretion rates not too far from the Eddington limit, the accretion radius r_a is close to the NS surface for magnetic moments $\sim 10^{26}$ G cm^3. The fact that the magnetic moments of millisecond binary pulsars cluster around this value (bearing in mind that the progenitors of these systems are believed to be low-mass X-ray binaries, which have accretion rates close to the Eddington value) seems to suggest that the accretion-induced field decay stops once r_a becomes comparable to the NS radius. For small values of the accretion radius, the accreting matter will no longer be funneled in a systematic way by the field to accrete onto the polar caps, but instead accretes all over the surface of the NS in a more or less random way. If, as proposed by these authors, it is the ordered accretion onto the polar caps that causes the magnetic moment to decay (see, in particular, Burderi et al. 1996), then the decay stops once r_a reaches R. Combining the expression for the accretion radius with the condition $r_a = R$, we obtained the bottom value of the magnetic moment as a function of the accretion rate and the NS radius and mass,

$$\mu_{\text{bot}} = 1.1 \times 10^{26}(\phi^{-7/4} R_6^{9/4} \dot{m}^{1/2} M^{1/4}) \text{ G cm}^3 . \quad (10)$$

The above formula shows that with the smaller NS radius predicted by softer equations of state, and for low enough accretion rates, the accretion-induced decay of a NS magnetic moment may be significant, resulting in a bottom value substantially below 10^{26} G cm^3.

3.2. *The Lifetime and Luminosity of a Potential Submillisecond Pulsar*

Camilo, Thorsett, & Kulkarni (1994) note that the inferred characteristic ages of most millisecond pulsars in the disk are rather high, in some cases exceeding the estimated age of the Galaxy. As they point out, this apparent paradox can in principle be explained by invoking a braking index value much higher than the canonical value of $n = 3$, for instance from gravitational radiation. In fact, in the context of the nonaxisymmetric instabilities discussed in § 2, gravitational radiation damping is likely to occur in the early stage of submillisecond pulsar evolution. This might result in a braking index value higher than the canonical one. If this is significant, submillisecond pulsars might in fact evolve rapidly into ordinary millisecond pulsars, making their detection in the submillisecond period range more difficult. On the other hand, in the context of the canonical braking index ($n = 3$) model, Camilo et al. (1994) proposed two alternative explanations for the age paradox: (a) that the observed millisecond pulsar were born with periods close to the observed ones, or (b) that there is a spontaneous field decay during the pulsar slowing-down phase. In both cases, the apparent age, $\tau_c = 0.5\,(P/\dot{P})$, would be an overestimate of the true age. Now, if we accept the idea of accretion-induced field decay, the entire observed pulsar sample could in principle be understood without invoking any subsequent spontaneous field decay, simply assuming that a fraction of pulsars in the sample are recycled (Phinney & Kulkarni 1994). So, in agreement with the idea of accretion-induced field decay, we propose to exclude hypothesis (b). We are left with hypothesis (a), that millisecond pulsars were born with periods close to the ones observed. If this is true, the crucial point is to understand (on the basis of a sensitive experiment) whether the present sample of observed period values is representative of the entire population (in which case we end up with the conclusion that submillisecond pulsars do not exist), or whether it

represents the tip of the iceberg of a larger population of objects having a significant spread in periods, including submillisecond periods. With this hypothesis, we might also hope that submillisecond pulsars (like millisecond pulsars) maintain periods close to their original ones over long enough timescales. In this case, their detection in the submillisecond period range should be possible. We will show in what follows how low values of the magnetic moment, potentially reachable in the context of the scenario sketched above, allow reasonably long submillisecond lifetimes.

The emission mechanisms for a radio pulsar are believed to be rotating magnetic dipole radiation and magnetospheric currents associated with the emission of relativistic particles, both depending on the angle i between the NS magnetic moment and the spin axis (Goldreich & Julian 1969). These two emission mechanisms compensate in such a way that the total energy emitted is nearly independent of i (Bhattacharya & van den Heuvel 1991). The bolometric luminosity associated with this emission is

$$L \propto \frac{\dot{P}}{P^3} = \frac{2}{3c^3}\,\mu^2\omega^4 = 3.85 \times 10^{35}\mu_{26}^2 P_{-3}^{-4}\ \text{ergs s}^{-1}\ , \tag{11}$$

where P_{-3} is the spin period in ms. During this process the rotational energy of the NS is consumed, i.e.,

$$-\frac{d(I\omega^2/2)}{dt} = -I\omega\dot{\omega} - \frac{\dot{I}\omega^2}{2} = \frac{2}{3c^3}\,\mu^2\omega^4\ , \tag{12}$$

where I is the moment of inertia of the NS. For angular speeds close to the centrifugal limit, the NS shows significant oblateness (as indicated by the values of the eccentricity reported in Table 1). The inclusion of these oblateness effects in the moment of inertia and in the gravitational self-energy of the NS has been studied in the context of the Maclaurin spheroids by Cowsik, Ghosh, & Melvin (1983). Their results show that the standard scenario, in which both the gravitational energy and the moment of inertia are assumed to be constant during the spin-down process, can be considered as a good upper limit for the period evolution in the initial phase, becoming indistinguishable from the real evolutionary track as the eccentricity decreases. In line with this, and neglecting the term $\propto \dot{I}$, we have $L \propto \dot{P}/P^3$, so that

$$P\dot{P} = 9.75 \times 10^{-24}(\mu_{26}^2 I_{45}^{-1})\ , \tag{13}$$

where I is measured in units of 10^{45} g cm^2. Integrating this relation, we find

$$P(t)^2 = P(t=0)^2 + 6.15 \times 10^{-16}(\mu_{26}^2 I_{45}^{-1} t_{\text{yr}})\ , \tag{14}$$

where t_{yr} is the time in years. If a NS is spun up by the accretion process below the millisecond limit, we can derive the time spent in the submillisecond range during the radio pulsar phase

$$\tau = 1.63 \times 10^9(1 - P_{-3i}^2)\mu_{26}^{-2} I_{45}\ \text{yr}\ , \tag{15}$$

where P_{-3i} is the initial spin period in milliseconds.

Assuming that the EOS allows for the stability of a submillisecond pulsar, and assuming that the accretion process is able to spin up the NS in the submillisecond period range, the detectability of such an object depends essentially on its luminosity and on its time spent as a pulsating submillisecond source. A first crude evaluation of the detectability of a potential submillisecond pulsar can be made on the basis of the nominal bolometric luminosity. During the spin-down phase, the bolometric luminosity decreases as P^{-4}, so adopting as a lower limit the bolometric luminosity L_{min} at the end of the submillisecond lifetime (i.e., for $P_{-3} \sim 1$), and for a moment of inertia $\sim 10^{45}$ g cm^3 and a NS radius $\sim 10^6$ cm, in Figure 3 we plot L_{min} and τ (for the soft neutron-matter EOS B, which gave a minimum period value of ~ 0.62 ms) against the bottom magnetic moment, μ_{bot}, and against the corresponding accretion rates derived from equation (10). For comparison, the bolometric luminosity of the pulsar with one of the lowest known μ, J0034$-$0534 (3.7×10^{34} erg s^{-1}), is also shown. As it is possible to see, quite low values of the magnetic moment are attainable for reasonable accretion rates. For these values, the time spent in the submillisecond phase is long enough to guarantee significant detection probabilities. Moreover, owing to the strong dependence on the spin period, for most of the submillisecond lifetime the corresponding bolometric luminosity is well above the L_{min} value, making the detection probability even higher.

Proszynski & Przyibicien (1985) found empirically that the observed 400 MHz luminosity of pulsars, L_{400}, can be fitted by a relation

$$\log(L_{400}) = \tfrac{1}{3}\log(\dot{P}/P^3) + A \tag{16}$$

were $A = 1.1$ for a sample of 275 pulsars. Kulkarni, Narayan, & Romani (1990) also noted that a similar relation would easily fit a sample of 11 recycled binary pulsars. Figure 4 shows the observed luminosity L_{400} of the current sample of 26 millisecond pulsars selected on the basis of the condition $P \leq 25$ ms, plotted as a function of the parameter $\dot{P}/P^3$. The dashed line corresponds to the original fit of Proszynski & Przyibicien (1985). The two dotted lines correspond respectively to $A = -0.48$ and $A = 2.43$ and were arbitrarily drawn in order to define a plausible region of the luminosity versus $\dot{P}/P^3$. The range of the $\dot{P}/P^3$ parameter

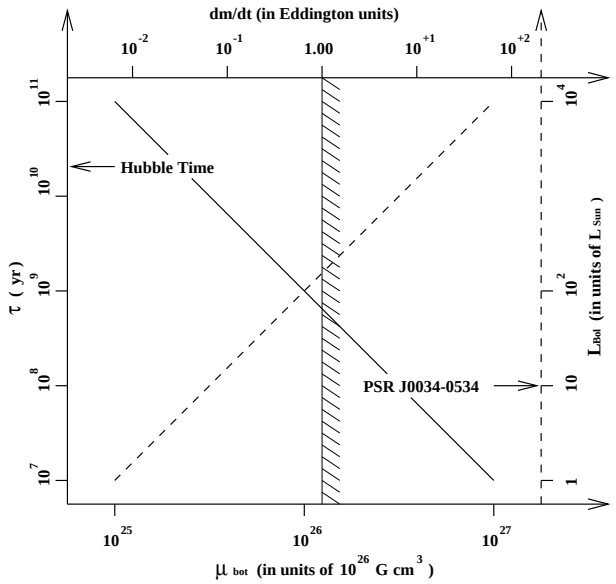

FIG. 3.—Submillisecond lifetime (*solid line*) and minimum bolometric luminosity (*dashed line*) (see text for definition) for a 0.62 ms pulsar (EOS B) vs. the bottom magnetic moment or the corresponding accretion rate. The bolometric luminosity of the sun is 3.83×10^{33} ergs s^{-1}, the Eddington accretion rate for a $R_6 \sim 1$ NS is $1.5 \times 10^{-8}\ M_\odot\ \text{yr}^{-1}$.

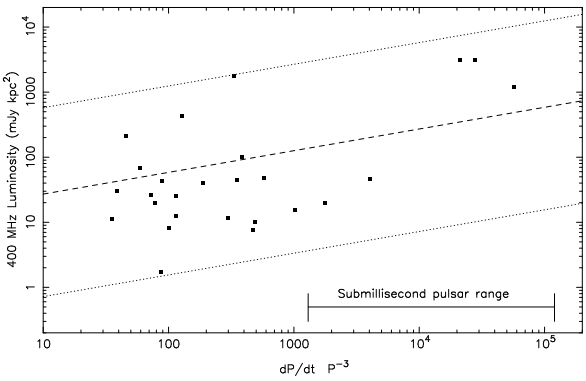

FIG. 4.—Observed 400 MHz luminosity, L_{400}, for 26 millisecond pulsars as a function of the parameter $\dot{P}/P^3$. The three lines represent the relation $\log L_{400} = \log (\dot{P}/P^3) + A$ for three different values of the parameter A (see text).

corresponding to a potential submillisecond pulsar with 0.6 ms $< P <$ 0.9 ms and 0.3×10^{26} G cm^3 $< \mu < 1.0 \times 10^{26}$ G cm^3 is also indicated in the figure. As can be seen, this is likely to correspond to a relatively high luminosity range.

On the basis of these empirical considerations, a submillisecond pulsar is potentially within the detection limit of most current surveys, provided that the system sensitivity is properly tuned in the submillisecond period range.

4. THE FEASIBILITY OF A SUBMILLISECOND PULSAR SEARCH

In this section we discuss the technical difficulties related to the detection of submillisecond pulsars, and the selection effects of the searches that have been conducted up to now. We show that the submillisecond period range has not been searched at the sensitivity level necessary to put firm upper limits to the limiting spin period of NSs.

The pulsed signal of a pulsar is dispersed by propagation in the ionized interstellar medium, and it must be sampled in both the time and frequency domains to be detected. The detectability of a pulsar of a given mean flux density depends on the pulsar period and the effective pulse width resulting from pulse smearing due to the discrete time and frequency sampling. For rapid dispersed pulsars, the minimum detectable mean flux density is given by (see, e.g., D'Amico 1997)

$$S_{\min} \propto \frac{k}{\sqrt{N_p \Delta\nu \Delta t}} \sqrt{\frac{w_e}{P - w_e}} \text{ mJy} , \quad (17)$$

where k is a factor that takes into account the sensitivity of the receiving system and depends on the receiver noise temperature and the antenna gain, N_p is the number of polarizations, $\Delta\nu$ is the observed bandwidth in MHz, Δt is the integration time in s, and w_e is the effective pulse width (in s), given by

$$w_e = \sqrt{w^2 + (\beta\,\delta t)^2 + \left(\frac{\text{DM}}{1.210^{-4}} \frac{\delta\nu}{\nu^3}\right)^2 + (\delta t_{\text{scatt}})^2} , \quad (18)$$

where w is the intrinsic pulse width, δt is the sampling time in s, β is a parameter that takes into account the effective time resolution as determined by the post-detection time constant and anti-aliasing filter (typically $\beta \simeq 2$), DM is the dispersion measure in pc cm^{-3}, $\delta\nu$ and ν are respectively the frequency resolution and the center observing frequency in MHz, and δt_{scatt} is the pulse broadening due to multipath scattering in the interstellar medium. This last term is roughly proportional to the dispersion measure, DM^2, and scales as ν^{-4}, so it can be minimized only with a proper choice of the observing frequency. In general, for pulsars away from the Galactic plane it is negligible.

So, from the technical point of view, the problem of the detection of rapid periodicities reduces to the conflict between the need to adopt a relatively large bandwidth $\Delta\nu$ and integration time Δt in order to achieve a given sensitivity limit, and the need to sample the two domains at high resolution. According to the above formulae, a sensitivity cutoff definitely occurs when the effective pulse width becomes comparable to the pulsar period; a significant loss of sensitivity is already known to occur when the effective duty cycle (defined as the ratio between the effective pulse width and the pulsar period) exceeds 50%. In this case, the nominal sensitivity is reduced by a factor of ≥ 3 (for an intrinsic duty cycle $w/P \leq 10\%$), compared to the most favorable case in which $w_e \simeq w$, and the pulsar signal, if detected, tends to appear more like a sinusoidal tone, typical of an interference. In fact, in the short period range, the measured sensitivity is usually worse than the theoretical sensitivity. Most search algorithms are optimized for the detection of sharp pulses. Even if nominally above the detection limit, highly dispersed pulses and periodicities in the period range of $\simeq 2$–4 sample intervals are usually unlikely to be recognized by the data processing algorithm as genuine pulsar signals, unless the observing and data processing strategies keep careful track of any sinusoidal spectral spike bearing a resemblance to most interferences. If we crudely assume that searches miss pulsars in the period range of ≤ 4 sample intervals, we must conclude that no searches sensitive in the submillisecond period range have been performed up to now, as essentially all the search experiments have used a sampling time $\delta t \geq 0.25$ ms.

The ability of a pulsar experiment to detect dispersed pulses is usually summarized by a parameter DM$_0$, the so-called diagonal DM, which represents the DM value corresponding to a pulse smearing of one time sample per frequency sample. Instead, in the following discussion we attempt to quantify the various experiments on the basis of their relative capacity to detect short periodicities for a given reference DM value.

Figure 5 shows the theoretical sensitivity of the major searches for millisecond pulsars, computed using the published experimental parameters. Figure 5*a* shows searches of the Galactic field with sensitivities computed adopting the mean DM value ($\simeq 26$ pc cm^{-3}) of the known field millisecond pulsars. Figure 5*b* shows searches of globular clusters. In this case, the DM value of individual cluster pulsars is used.

This figure shows very clearly that the relative exposure to the submillisecond period range has always been poor. As we mentioned before, the actual sensitivity in the ultrashort period range is in most cases even worse. In order to characterize the relative ability of each experiment to detect short period pulsars, we define a parameter P_{65}(DM) as the period value corresponding in equation (18) to a pulse smearing of 65% of the pulsar period. Table 2 lists the relevant experimental parameters for the Galactic field and globular cluster searches, respectively. The first column gives the experiment name (or the cluster name), the next six

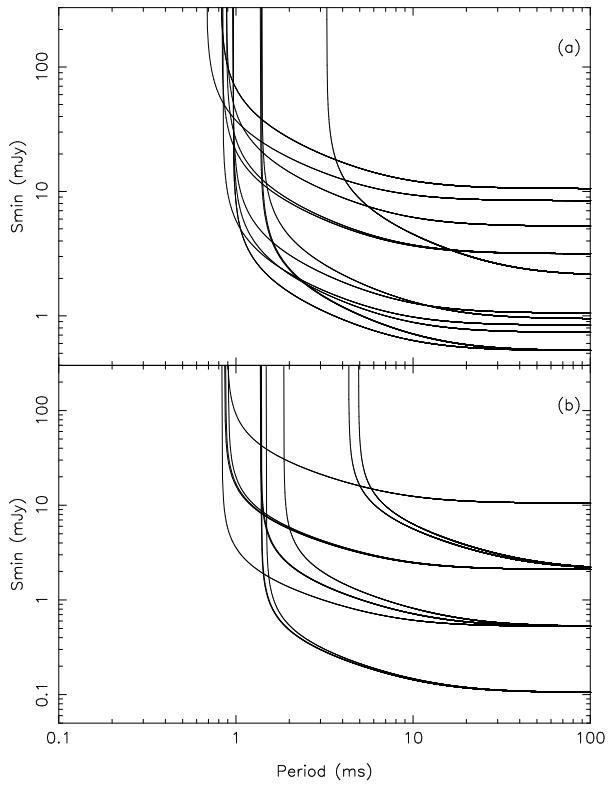

FIG. 5.—(*a*) Minimum detectable mean flux density for the major searches of the Galactic field for millisecond pulsars. A mean DM reference value of 26 pc cm^{-3} is assumed. (*b*) Minimum detectable mean flux density for the major searches of globular clusters for millisecond pulsars. For each cluster, the measured DM value of the known cluster pulsars is used (see Table 2).

columns give the sampling time δt, the frequency resolution δv, the center frequency v, the integration time Δt, the total bandwidth Δv, and the minimum detectable mean flux density for long period pulsars, S_0. The seventh column gives the P_{65} parameter, computed adopting the DM value quoted in column eight. As in Figures 5*a* and 5*b*, for the Galactic field searches a mean reference value of DM $\simeq$ 26 was used, while for globular cluster searches the DM value of the individual cluster pulsars was used. As can be see from the tables, in most cases the P_{65}(DM) parameter is above 1 ms, except in two of the four high-frequency experiments where, on the other hand, the intrinsic sensitivity was not very high. So, apart perhaps from a fairly small local volume of the Galactic field corresponding to DM $\ll$ 26 pc cm^{-3} (for instance, for DM = 5 pc cm^{-3}, the P_{65}(DM = 5) value of the Arecibo-CBHL experiment is $\simeq$0.6 ms), the Galaxy has been poorly searched for pulsars in the submillisecond period range.

Most experiments to date have used a relatively large total bandwidth and integration time, so that the intrinsic sensitivity (or the sensitivity for long period pulsars) was relatively high. However, the sensitivity in the submillisecond period range was rather poor. In fact, sampling the same frequency and time domains with much higher resolutions would have been prohibitive in terms of data storage and computing capacity. Of course, this compromise had its advantages, as a large sample of new ordinary pulsars has been detected in addition to a (still growing) number of millisecond pulsars. On the other hand, the possibility of probing the EOS of ultradense matter was not touched on by these experiments.

It is worth noting that experiments like the Parkes All Sky Survey produced about a terabyte of data and required supercomputing facilities to reduce the survey data. The only way to significantly improve the sensitivity in the submillisecond period range without exacerbating the data storage and data processing requirements is to sacrifice the total bandwidth and the integration time, resulting in a much lower sensitivity in the long period range. With a proper choice of observing system parameters, this corresponds to tilting the curves in Figure 5, gaining sensitivity in the ultrashort period range while losing it in the long period range. With current hardware and software resources, a sensitive search of the submillisecond period range can be carried out only as a dedicated project, and not as the tail of a search tuned to a different volume of the pulsar parameter space.

The choice of the observing frequency for such experiments may need discussion. Large-scale surveys of the Galactic field for millisecond pulsars at relatively low frequencies ($\simeq$400 MHz) have proven successful. The progenitors of millisecond pulsars are old binary systems, so millisecond pulsars are expected to be found also at high Galactic latitudes. At low frequencies, the telescope beams tend to be wider, making a high-latitude search more feasible, and the sky background temperature away from the Galactic disk is relatively low. Pulsars, and in particular millisecond pulsars, have steep spectra, so they are more easily detected at meter wavelengths. So if the population of submillisecond pulsars is similar to the millisecond pulsar population in Galactic distribution and luminosity, a systematic high-latitude search at 400 MHz with enough time and frequency resolution (say $\delta t \leq 100$ μs and $\delta v \leq 50$ kHz) should be successful. On the other hand, if submillisecond pulsars are very rare objects, on average their distance will be very high, so they will need to be searched for at low Galactic latitude, deep in the Galactic disk. In this case, only a relatively high-frequency experiment ($\simeq$1.4 GHz) will do the job.

A new low-frequency experiment with a rather low value of the P_{65}(DM) parameter is in progress at Bologna (D'Amico 1997). New high-frequency experiments (1.4 GHz) using a short sampling interval are planned at Jodrell Bank and Parkes. It is to be hoped that before the next century, the limiting spin period of NSs will be observationally determined, and the EOS of ultradense matter can be tested.

5. CONCLUSION

The detection of a submillisecond pulsar would be a unique tool to probe the EOS of dense matter. We have shown that submillisecond pulsars might not be so rare. In the context of the standard millisecond pulsar formation process, the spin-up equilibrium period corresponding to the end of the accretion-induced spin-up phase in recycled pulsars can easily be below 1 ms. This model is thus potentially efficient in producing submillisecond pulsars. Some models of accretion-driven magnetic field decay would give a submillisecond pulsar a magnetic moment low enough to guarantee a relatively long spin-down timescale. In spite of the predicted low field, such a fast rotating NS would have a bolometric luminosity comparable to or even higher than that commonly observed in millisecond pulsars. In principle, we may expect these objects to be observable as pulsa-

TABLE 2

EXPERIMENTAL PARAMETERS

SEARCHES OF THE GALACTIC FIELD

Experiment name	δt (ms)	$\delta \nu$ (MHz)	ν (MHz)	Δt (s)	$\Delta \nu$ (MHz)	S_0 (mJy)	P_{65}(DM) (ms)	DM_{ref} (pc cm^{-3})	Reference
Arecibo HL-6	0.25	0.250	430	33	8	0.5	1.3	26	1
Arecibo HL-2-5	0.25	0.250	430	33	8	0.5	1.3	26	2
Arecibo HL-1	0.5	0.080	430	40	10	0.5	1.6	26	3
Arecibo SHL	0.25	0.250	430	8	8	1.	1.3	26	4
Arecibo DHL	0.25	0.250	430	32	8	0.7	1.3	26	4
Arecibo AC	0.506	0.080	430	67	10	0.5	1.6	26	4
Arecibo CBHL	0.180	0.250	430	47	8	0.8	1.2	26	5
Arecibo GP	0.51	0.080	430	67	10	0.9	1.6	26	6
Princeton-Arecibo	0.3	0.060	430	39	1	3	1.0	26	7
Parkes 2	0.3	0.125	430	157	32	3	1.1	26	8
Parkes 1*b*	0.3	1.	1400	157	80	3	0.9	26	9
Parkes 1*a*	1.2	5.	1400	157	320	1	3.7	26	9
Jodrell HL	0.3	0.125	430	320	8	4	1.1	26	10
Jodrell GP	2.0	5.	1400	157	40	2	6.2	26	11
Molonglo	0.25	0.125	843	120	4	8	0.8	26	12

SEARCHES OF GLOBULAR CLUSTERS

Cluster name	δt (ms)	$\delta \nu$ (MHz)	ν (MHz)	Δt (s)	$\Delta \nu$ (MHz)	S_0 (mJy)	P_{65}(DM) (ms)	DM_{ref} (pc cm^{-3})	Reference
47 Tucanae	0.3	0.250	650	2500	32	0.5	1.0	24.	13
M53	0.506	0.080	430	5400	10	0.1	1.6	24.	14
M5	0.506	0.312	1400	5400	40	0.5	1.6	29.5	15
M4	0.3	0.125	610	320	4	2.	1.0	62.9	16
M13	0.506	0.080	430	5400	10	0.1	1.6	30.	17
NGC 6342	0.3	0.125	610	320	4	2.	1.1	70	18
NGC 6440	0.3	0.25	650	2500	32	0.5	2.7	220	19
Terzan 5	1.2	5.	1400	2500	320	2	6.8	242	20
NGC 6539	1.2	5.	1400	2500	320	2	5.7	187	21
NGC 6624	0.3	0.125	610	320	4	2	1.1	87	22
M28	0.3	1.	1400	5000	32	10	1.1	120	23
NGC 6760	0.506	0.312	1400	4200	40	0.5	1.6	200	24
M15	0.506	0.080	430	5400	10	0.1	1.8	67	25

REFERENCES.— (1) Camilo, Nice, & Taylor 1996; (2) Foster et al. 1995; (3) Wolszczan 1991; (4) Ray et al. 1995; (5) Thorsett et al. 1993; (6) Nice, Fruchter, & Taylor 1995; (7) Stokes et al. 1986; (8) Manchester et al. 1996; (9) Johnston et al. 1992; (10) Nicastro et al. 1995; (11) Clifton et al. 1992; (12) D'Amico et al. 1988; (13) Manchester et al. 1991; (14) Kulkarni et al. 1991; (15) Wolszczan et al. 1989; (16) Lyne et al. 1988; (17) Anderson et al. 1990a; (18) Biggs, Lyne, & Johnston 1989; (19) Lyne, Manchester, & D'Amico 1996; (20) Lyne et al. 1990; (21) D'Amico et al. 1993; (22) Biggs et al. 1994; (23) Lyne et al. 1987; (24) Middleditch et al. 1991; (25) Anderson et al. 1990b.

ting radio sources. However, the submillisecond period range has not yet been searched. With the present generation of data processing facilities, the only way to search this range in a large-scale survey is to sacrifice the sensitivity to long-period pulsars and to tune the hardware and software parameters to resolve pulses as narrow as $< 100\ \mu$s.

We gratefully acknowledge financial support from the Italian Ministero dell' Università e della Ricerca Scientifica e Tecnologica and the UK Particle Physics and Astronomy Research Council.

We also thank an anonymous referee for very interesting comments and suggestions.

REFERENCES

Anderson S. B., et al. 1990a, Bull. Am. Phys. Soc., 22, 1285
———. 1990b, Nature, 346, 42
Arnett, W. D., & Bowers, R. L. 1977, ApJS, 33, 415
Bhattacharya, D., & Srinivasan, G. 1995, in X-Ray Binaries, ed. W. H. G. Lewin, J. van Paradijs, & E. P. J. van den Heuvel (Cambridge: Cambridge Univ. Press), 495
Bhattacharya, D., & van den Heuvel, E. P. J. 1991, Phys. Rep., 203, 1
Bhattacharya, D., Wijers, R. A. M., Hartman, J. W., & Verbunt, F. 1992, A&A, 254, 198
Biggs, J. D., Lyne, A. G., & Johnston, S. 1989, in Proc. 23d ESLAB Symp., Vol. 1: X Ray Binaries (Paris: ESA), 293
Biggs, J. D., et al. 1994, MNRAS, 267, 125
Bisnovatyi-Kogan, G., & Komberg, B. 1974, Soviet Astron., 18, 217
Blondin, J. M., & Freese, K. 1986, Nature, 232, 786
Burderi, L., King, A. R., & Wynn, G. A. 1996, MNRAS, 283, L63
Camilo, F., Nice, D. J., & Taylor, J. H. 1996, ApJ, 461, 812
Camilo, F., Thorsett, S. E., & Kulkarni, S. R. 1994, ApJ, 421, L15
Chandrasekar, S. 1970a, Phys. Rev. Lett., 24, 611
———. 1970b, ApJ, 161, 561
Clifton, T. R., Lyne, A. G., Jones, A. W., McKenna, J., & Ashworth, M. 1992, MNRAS, 254, 177
Comins, N. 1979a, MNRAS, 189, 233
———. 1979b, MNRAS, 189, 255
Cook, G. B., Shapiro, S. L., & Teukolsky, S. A. 1994, ApJ, 424, 823
Cowsik, R., Ghosh, P., & Melvin, M. A. 1983, Nature, 303, 308
Cutler, C., & Lindblom, L. 1987, ApJ, 314, 234
Cutler, C., Lindblom, L., & Splinter, R. J. 1990, ApJ, 363, 603
D'Amico, N. 1997, Proc. NATO ASI, The Many Faces of Neutron Stars, in press
D'Amico, N., et al. 1988, MNRAS, 234, 437
———. 1993, MNRAS, 260, L7
Detweiler, S., & Lindblom, L. 1985, ApJ, 292, 12

Foster, R. S., Cadwell, B. J., Wolszczan, A., & Anderson, B. S. 1995, ApJ, 454, 826
Friedman, J. L. 1983, Phys. Rev. Lett., 51, 11
Friedman, J. L., & Ipser, J. R. 1992, Philos. Trans. R. Soc. London, 340, 391
Friedman, J. L., Ipser, J. R., & Parker, L. 1986, ApJ, 304, 115
Glendenning, N. K. 1992, Phys. Rev. D, 46, 4161
Goldreich, P., & Julian, W. H. 1969, ApJ, 157, 869
Imamura, J., Durisen, R., & Friedman, J. L. 1985, ApJ, 294, 474
Johnston, S., et al. 1992, MNRAS, 255, 401
Koranda, S., Stergioulas, N., & Friedman, J. L. 1997, ApJ, 488, in press
Kulkarni, S. R. 1986, ApJ, 306, L85
Kulkarni, S. R., Anderson, S. B., Prince, T. A., & Wolszczan, A. 1991, Nature, 349, 47
Kulkarni, S. R., Narayan, R., & Romani, R. W. 1990, ApJ, 356, 174
Lindblom, L. 1986, ApJ, 303, 146
———. 1987, ApJ, 317, 325
Lindblom, L., & Detweiler, S. L. 1977, ApJ, 211, 565
Lyne, A. G., et al. 1987, Nature, 328, 399
———. 1988, Nature, 332, 45
———. 1990, Nature, 347, 650
Lyne, A. G., Manchester, R. N., & D'Amico, N. 1996, ApJ, 460, L41
Managan, R. 1985, ApJ, 294, 463
Manchester, R. N., et al. 1991, Nature, 352, 219
———. 1996, MNRAS, 279, 1235
Mendell, G. 1991, ApJ, 380, 530
Middleditch, J., et al. 1991, Bull. Am. Phys. Soc., 23, 1348
Nicastro, L., et al. 1995, MNRAS, 273, L68
Nice, D. J., Fruchter, A. S., & Taylor, J. H. 1995, ApJ, 449, 156
Ostriker, J. P., & Gunn, J. E. 1969, ApJ, 157, 1395
Pandharipande, V. R. 1971, Nucl. Phys. A, 178, 123
Pandharipande, V. R., & Smith, R. A. 1975, Nucl. Phys. A, 175, 225
Phinney, E. S., & Kulkarni, S. R. 1994, ARA&A, 32, 591
Proszynski, M., & Przybycien, D. 1985, in Workshop on Millisecond Pulsars, ed S. P. Reynolds & D. R. Stinebring (Green Bank: NRSO), 151
Ray, P. S., et al. 1995, ApJ, 443, 265
Romani, R. W. 1990, Nature, 347, 741
Sang, Y., & Chanmugam, G. 1987, ApJ, 323, L61
Shapiro, S. L., & Teukolsky, S. A. 1983, Black Holes, White Dwarfs, and Neutron Stars (New York: Wiley)
Shibazaki, N., Murakami, T., Shaham, J., & Nomoto, K. 1989, Nature, 342, 656
Stergioulas, N., & Friedman, J. L. 1995, ApJ, 444, 306
Stokes, G. H., Segelstein, D. J., Taylor, J. H., & Dewey, R. J. 1986, ApJ, 311, 694
Taam, R. E., & van den Heuvel, E. P. J. 1986, ApJ, 305, 235
Taylor, J. H., & Weisberg, J. M. 1989, ApJ, 345, 434
Thomson, W., & Tait, P. G. 1883, Principles of Natural Philosophy (Oxford: Clarendon)
Thorsett, S. E., Deich, W. T. S., Kulkarni, S. R., Navarro, J., & Vasisht, G. 1993, ApJ, 416, 182
Urpin, V. A., & Muslimov, A. G. 1992, MNRAS, 256, 261
van den Heuvel, E. P. J. 1995, JApA, 16, 255
van den Heuvel, E. P. J., & Bitzaraki, O. 1994, Mem. Soc. Astron. Italiana, 65, 237
Wakatsuki, S., Hikita, H., Sato, N., & Itoh, N. 1992, ApJ, 392, 628
Witten, E. 1984, Phys. Rev. D, 30, 272
Wolszczan, A. 1991, Nature, 350, 688
Wolszczan, A., Anderson, S., Kulkarni, S. R., & Prince, T. 1989, IAU Circ. No. 4880, 1